**Supporting Information:**

Supporting Text 1: Nomenclature for the number of motors moving beads.

There has been theoretical work investigating how multiple motors are expected to function together (Ref. 9). Unfortunately, comparing theory and experiment is not straightforward. In the theoretical work (Ref. 9), the cargo was assumed to be driven by a single group of motors, attached to the cargo at a single point. Thus, assays were classified based on the maximum number of motors participating in transport – a scheme which is optimal when cargos have a fixed number of motors geometrically available for active transport. This constraint is not valid for our assays (see below) and so the scheme in Ref. 9 is inconvenient for us.

At low kinesin concentrations, motors on the bead are so sparse, that any time the bead is moved, only one motor is able to reach the microtubule. However, as the kinesin concentration increases, there is an increasing probability that some of the time the bead will be moved by two motors located close enough to each other to work together. However, the fraction of time that this is true is a function of the kinesin concentration: at lower concentrations, on a given bead there are likely many individual active kinesins that could move the bead, but only a few of those are close enough to a second motor that the two motors could engage simultaneously. Thus if the actively transported bead happens to be moved by one of the isolated motors it would be a 'one motor bead', otherwise it would be a "two motor bead" (or perhaps "three motor bead", etc.). This illustrates the main problem with using the notation in Ref. 9 for our assay classification: the number of motors geometrically available for active transport can vary from bead to bead and even for a given bead, depending on when the measurement is made. Because

of this difficulty, we have chosen a convention where we characterize the population statistically, as described in the main text. Therefore, due to the differences in the experiments versus theory, our shorthand assay designations (1,~2,3+ motor assays) are different from the designations in Ref. 9.

Supporting Text 2: The effective 'on rate' depends on kinesin concentration.

We expect the on rate to be a function of the density of kinesins on the bead. Consider for instance a situation where one kinesin motor is bound to the microtubule. It is possible that there are several other motors that are close enough to the bound motor to reach the microtubule, yet are far enough from each other that they cannot be active simultaneously. In this situation, the effective on-rate will be several times the actual on-rate for each un-attached motor, because as the bead (still tethered to the MT via one kinesin molecule) rotates, any one of the other available motors can rebind. Notice that, although the force measurements indicate that, when the bead was stalled, it was typically moved by 2 kinesins, the force measurements do not tell us how many different combinations of 2 kinesins there were that could work together. The on-rate is thus a function of the number of available motors which itself depends on motor density on the cargo.

Our experimental evidence indicates that the effective on-rate increases with motor concentration: compare the on-rate for the low-kinesin bead to that of the higher kinesin bead (Fig 2, main text): the typical time between motile events (reflecting the effective on rate) for the low-kinesin bead is roughly half that for the higher kinesin bead. At high kinesin concentrations (typical of the ~2 motor assay) the bead is almost always

in motion, so the on rate is harder to estimate but is obviously higher still. Ultimately, variations in local motor arrangement for a given bead and across the bead population in a given assay, combined with the fact that the effective on rate is not constant across assays, but increases with motor concentration, makes quantitative comparison between the previously published theory and our experiments difficult.

Figure 6. Schematic illustrating the effect of increasing incubation concentration on kinesin density on beads. Beads incubated with low amounts of kinesin have only one motor attached to their surface (a). As the incubation concentration increases, the spacing between attached motors decreases (b-d). Consequently, the probability that a motor bound to a MT will have no neighbors that could reach the MT decreases. Note also that at high motor densities on beads, several such neighboring motors may be able to reach the MT, which is likely to increase the observed motor on-rate.

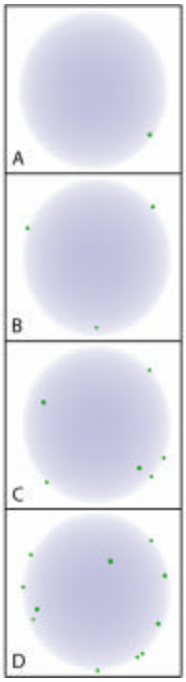


Fig. 6

Figure 7. The effect of tau and kinesin concentrations on bead-MT binding. (a) The effect of changing kinesin concentrations for several fixed tau concentrations. Polystyrene beads were incubated with varying amounts of kinesin-I motors and subsequently tested for binding to MTs (see above). The fractions of binding events are shown for bound 4RL tau:tubulin ratios of 0, 0.123, 0.238 for various molar motor:bead ratios ($n$). The error bars shown are estimated as $\sqrt{P(1?P)/N_{total}}$, where $P$ is the fraction of binding events and $N_{total}$ is the number of beads tested. Solid lines are fits to the single molecule Poisson distribution $P(n)?1?e^{?n/b}$, both for bare and tau-decorated MTs. Increasing tau depresses the binding fraction at particular kinesin:bead ratios (binding affinities $b$ = 213.4 ± 22.2 , 452.7 ± 43.0, 3081.3 ± 301.8 for the 4RL tau:tubulin ratios of 0, 0.123, 0.238 respectively, and $b$=3498.7 ± 325.4 for the 3RS tau:tubulin ratio of 0.107). The arrow indicates the kinesin concentration at which the switching experiments (see above) were conducted. (b) The effect of changing tau concentration for a fixed kinesin concentration. The binding fraction at constant motor concentration (binding fraction on bare MTs of 0.7 ± 0.05) but varying bound tau amounts is shown for 3RS tau and 4RL tau (the curves are normalized to their values on bare MTs). The midpoints extracted from the sigmoid fits (solid lines) are $x_o$ = 0.050 ± 0.002 and 0.192 ± 0.002 for 3RS tau and 4RL tau respectively. (c) The binding curves (20) for the two tau isoforms used in this study (3RS tau and 4RL tau) are shown. The measurements reported in (a) were performed at tau:tubulin ratios indicated by arrows. The measurements reported in (b) were performed at tau:tubulin ratios indicated by circles.

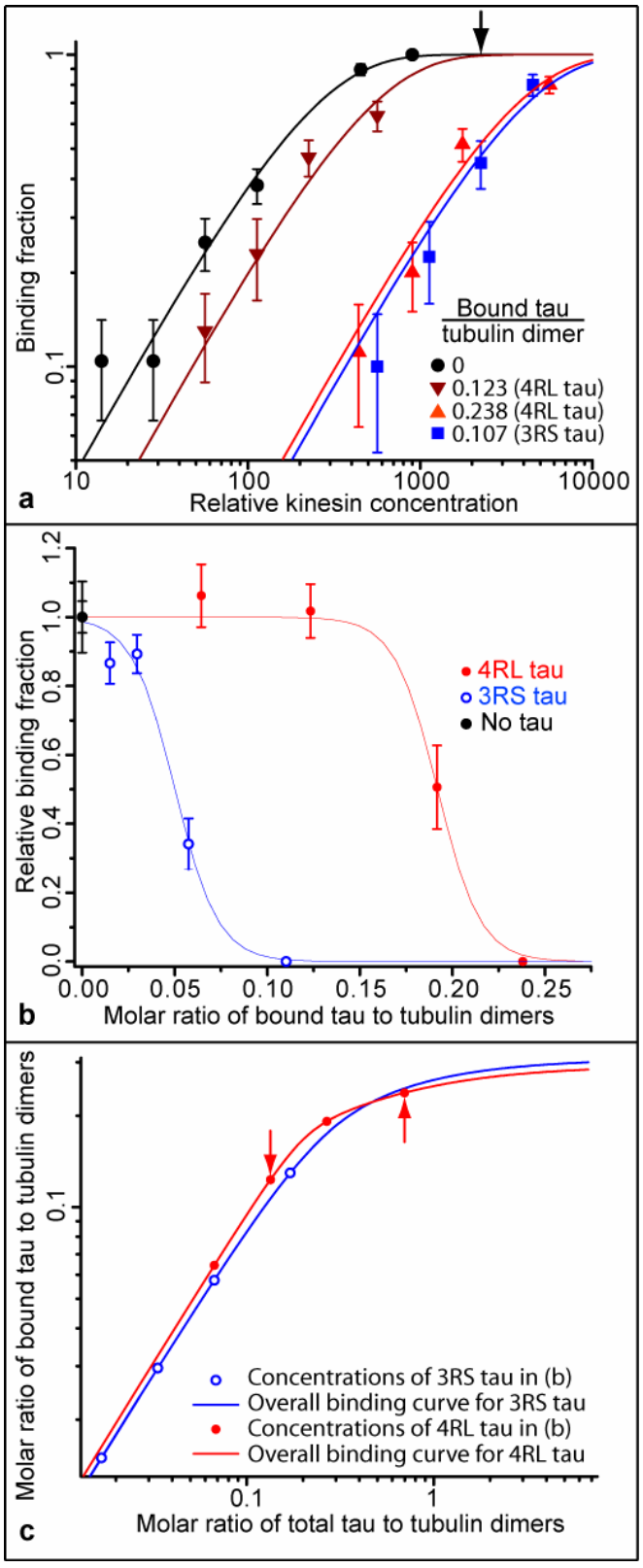
Binding fraction
1
0.1
10
100
1000
10000
Relative kinesin concentration
a
Bound tau
tubulin dimer
0
0.123 (4RL tau)
0.238 (4RL tau)
0.107 (3RS tau)
Relative binding fraction
0.0
0.2
0.4
0.6
0.8
1.0
1.2
0.00
0.05
0.10
0.15
0.20
0.25
Molar ratio of bound tau to tubulin dimers
b
4RL tau
3RS tau
No tau
Molar ratio of bound tau to tubulin dimers
0.1
0.1
1
Molar ratio of total tau to tubulin dimers
c
Concentrations of 3RS tau in (b)
Overall binding curve for 3RS tau
Concentrations of 4RL tau in (b)
Overall binding curve for 4RL tau

Fig. 7

Figure 8. Western blot quantification of tau binding to microtubules (see Materials and Methods for further details). Microtubule bound fractions of 4RL (lane I) and 3RS (lane II) tau are compared with reference dilutions of 4RL (lane III) and 3RS (lane IV) tau. In all cases the starting amount of tau in an assay was the same (1.4 ? M). In the cosedimentation assays, the ratio of total tau to tubulin dimers was 0.072, substantially below the binding saturation turnover. Approximately 90% of the 4R tau and 87% of 3R tau was found to be competent to bind microtubules as determined by quantitative densitometry analysis, confirming the tight binding of both isoforms of tau to MTs. In accordance with previous results (20), the 4RL isoform attaches slightly more readily in our assay conditions. Therefore the stronger effect of 3RS tau upon kinesin-based transport reported in this work is not due to more 3RS tau attaching to the MTs under identical incubation conditions.

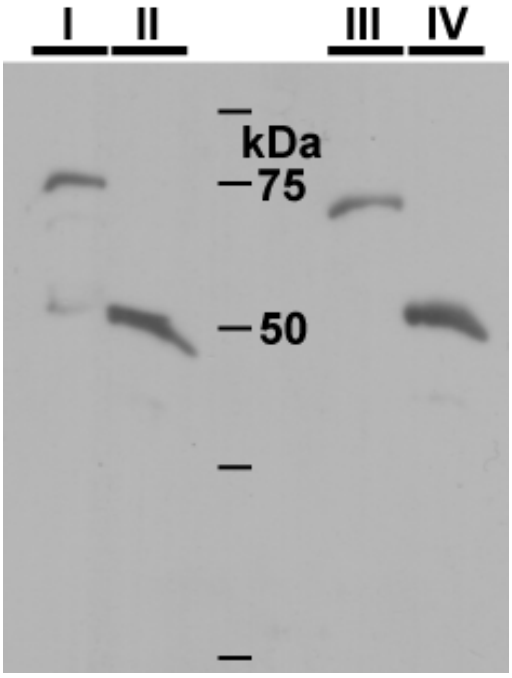


Figure 8.

Figure 9. A schematic diagram of the flow cell. Grey areas represent walls of the flow cell (made from double-sided tape gluing the glass parts of the flow cell together). Top and side views are shown.

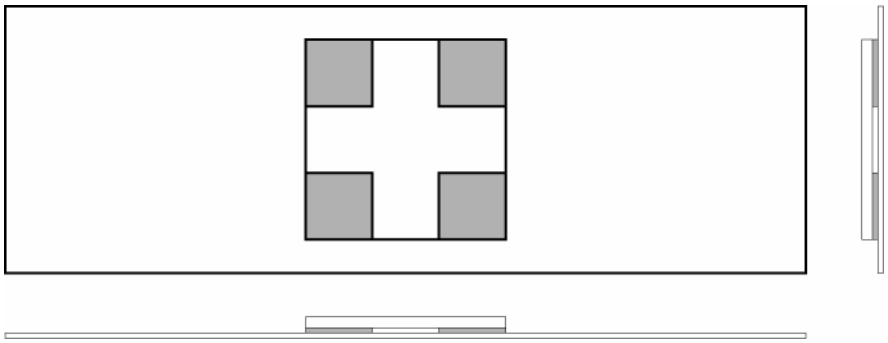

Figure 9.

Figure 10. A processed excerpt of video recording, showing the crossed microtubule arrangement. For clarity, 10 consecutive frames were spatially blurred to reduce point to point visual noise and averaged. The microtubules were imaged using differential interference contrast (DIC) microscopy. The bead is seen near the center of the image. Small circular blemishes are optical obstructions at the camera and do not represent any features in the assay.

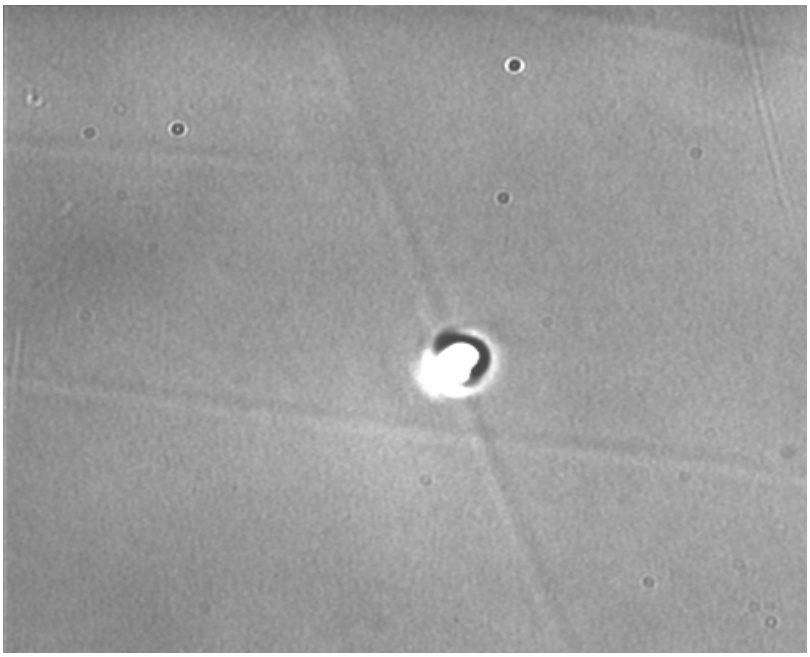

Figure 10.

Figure 11. Force traces corresponding to one (a) and those we attribute to two (b) motor stalling events are shown. As beads are incubated with increased kinesin concentrations, the rate of binding events goes up, so that eventually such events are no longer always cleanly separated from each other. Thus, perhaps counter-intuitively, obtaining clean stall force records is more challenging at high incubation concentrations.

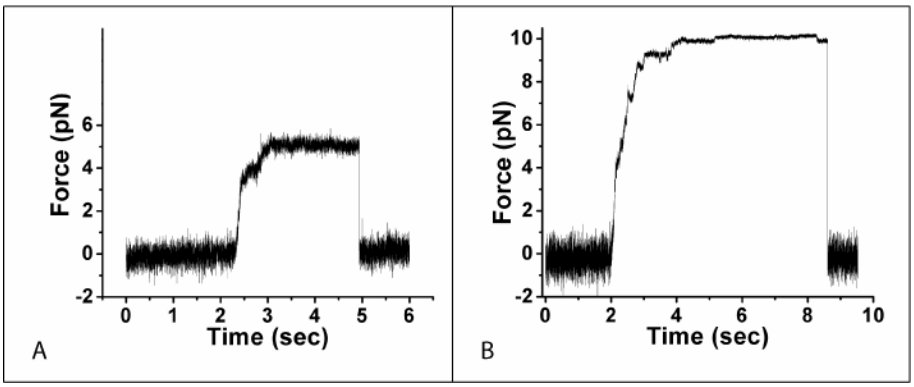


Fig. 11

Figure 12. Purification of Tau and kinesin. (a) Recombinant 3R and 4R tau proteins were purified, separated by SDS-PAGE, and stained with Coomassie blue. (b) Kinesin was purified from bovine brain, separated by SDS-PAGE, and stained with Coomassie blue. Purified bovine kinesin is comprised of two kinesin heavy chains and two light chains per molecule. The bovine heavy chains run as a single band and the bovine light chains run as a doublet of ~50-60 kDa light chains (1-3).


1. Balczon, R., Overstreet, K. A., Zinkowski, R. P., Haynes, A. & Appel, M. (1992) *Endocrinology* **131,** 331-6.
2. Cyr, J. L., Pfister, K. K., Bloom, G. S., Slaughter, C. A. & Brady, S. T. (1991) *Proc Natl Acad Sci U S A* **88,** 10114-8.
3. Verhey, K. J., Lizotte, D. L., Abramson, T., Barenboim, L., Schnapp, B. J. & Rapoport, T. A. (1998) *J Cell Biol* **143,** 1053-66.


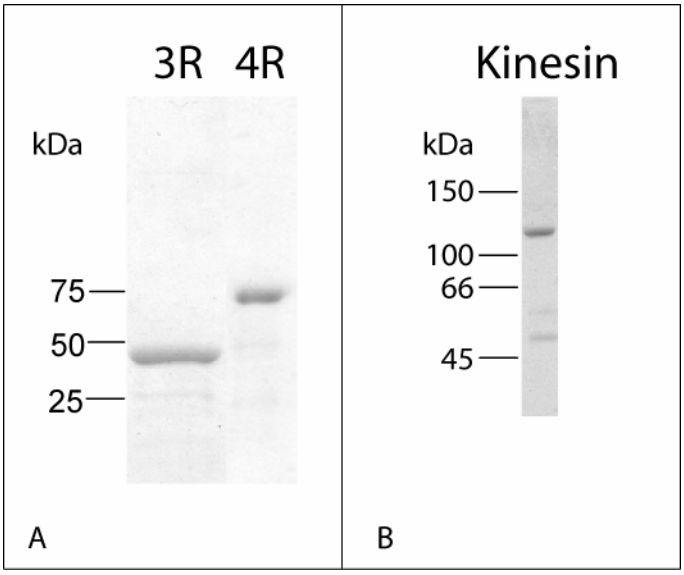


Fig. 12

Movie 1. The movie starts with a bead being held in an optical trap. Once it starts to move processively, the trap is turned off allowing the bead to move for a short distance. The bead detaches after approximately 1.6 ? m of travel. This type of motion is typical for beads incubated with low kinesin concentrations.

Movie 2. The movie shows a bead being deposited on the microtubule and moving processively across the entire field of view. This type of motion is characteristic of ~2 motor assay (as well as assays with higher motor concentrations). The robustness of transport we observe in our ~2 motor assay may appear surprising in light of the existing theoretical predictions(9). However, in our ~2 motor assay we do observe some activity consistent with a contribution from a third motor. Such events would correspond to three motor case of Ref. 9 and one would expect increased persistence for those cases. Additionally, we stabilize the beads near a microtubule to enable them to bind before releasing the beads and measuring their persistence. This may allow several motors to be bound at the outset of motion. Such initial conditions can be expected to suppress short travel events, improving apparent transport robustness. Lastly, the kinesin binding and rebinding constants may be different than those used in Ref. 9.

Movie 3. A 200 nm diameter polystyrene bead (~2 motor assay incubation conditions) moves across the entire field of view (~16 micron) illustrating the robust multiple-motor based transport on bare MTs. Thus, our results are likely relevant for a wide variety of

cargos and sizes, including essentially the entire range of cellular cargo sizes, so long as the cargos are large enough to be moved by multiple kinesin motors.